

The Application of Classical POD and Snapshot POD in a Turbulent Shear Layer with Periodic Structures[†]

D. HILBERG, W. LAZIK and H.E. FIEDLER*

Hermann-Föttinger-Institut, Technische Universität Berlin, Germany (author for correspondence)*

Received 8 September 1993; accepted in revised form 15 February 1994

Abstract. The classical and snapshot proper-orthogonal-decomposition was applied to data taken in a one-stream mixing layer in a narrow channel. Due to this particular geometry the flow develops large periodic structures. POD-analysis of simultaneously measured velocity components in spanwise direction identify as largest mode not only their periodic fraction, but also higher Fourier modes of the two-dimensional fluctuation. The energy content of the plane motion reaches values of about 90%. The amplitude of small three-dimensional vortices embedded in higher POD modes is correlated with the phase of the large structures, which indicates their influence on the entire turbulent motion. Application of scalar snapshot POD on phase averaged data of the entire flow field allows separation into modes. The eigenvalues and eigenvectors show identical distribution for the u' - and v' -component. Comparison of streakline plots of the reconstructed velocity field from different numbers of modes with flow visualization exhibits that the largest physical structure is described by only the first two modes. This is also supported by calculation of the vorticity component in z -direction. The total energy content of the largest structure is approximately 60%.

1. Introduction

The classical POD as introduced by Lumley (1967, 1981) and Sirovich (1989) and the snapshot POD suggested by Sirovich (1987) and Sirovich and Kirby (1987), both based on the Karhunen–Loeve expansion (Loeve, 1955), were applied to hot-wire measurements taken in the turbulent region of a one-stream mixing layer with small sidewall distances B , where B is typically less 1/10 of the test section of length L . Due to this geometry this flow develops periodic structures of large scale corresponding to the test section length. The periodicity is caused by the feedback of coherent acoustic waves originating at the trailing edges of the two sidewalls, when a dominating structure leaves the test section. These waves travel upstream, where they trigger a new wave at the trailing edge of the mixing layer. Accordingly, the Fourier spectrum shows a strong peak with a periodic fraction of about 30–45% of the total u' -value. Correlation measurements and flow visualization in spanwise direction exhibit the two-dimensionality of the periodic motion (Hilberg and Fiedler, 1989; Fiedler and Hilberg, 1992).

[†] Supported by the Deutsche Forschungsgemeinschaft under Grant No. Fi 178/28.

2. The Classical and Snapshot POD Method

The POD methods applied here are based on a scheme suggested by Glezer et al. (1989). Assuming u' -fluctuations to be measured simultaneously at M -positions in space and at N -points in time, the time series of the data is to be combined in a matrix A as columns $a^{(i)}$

$$A = u'_{ij} \quad i = 1, 2, \dots, M; j = 1, 2, \dots, N$$

$$a^{(i)} = (u'_{i1}, u'_{i2}, \dots, u'_{iN}) \quad i = 1, 2, \dots, M.$$

For optimal representation of the time series an orthogonal basis Ξ is searched, for which the mean quadratic scalar-product

$$\xi^{(k)} = \sum_{i=1}^M (a^{(i)} \cdot \Xi^{(k)})^2 \quad k = 1, 2, \dots, M$$

is maximized. This leads to an eigenvalue problem

$$(A^T A) \Xi^{(k)} = \xi^{(k)} \Xi^{(k)} \quad k = 1, 2, \dots, M.$$

EISPACK routines were used for the numerical solution and decomposition of the signals into orthogonal POD modes of number M . The corresponding eigenvalues ξ denote the energy content. The flow field corresponding to a POD mode is calculated from

$$\langle u' \rangle^{(k)} = a_t^{(k)} \Xi^{(k)}, \quad k = 1, 2, \dots, M,$$

$$a_t^{(k)} = A \Xi^{(k)},$$

where the coefficients a_t are functions of time only. Summation over the flow-fields allows the reconstruction of the original velocity field.

This method is known as the classical POD. By exchanging rows and columns of the matrix A the snapshot POD is obtained, where one column corresponds to one instantaneous 'snapshot' of the flow field. In this case then, the eigenvectors Ξ are functions of time and the coefficients a_t are functions of space.

3. Application of Classical POD

The classical POD method was applied to u' -time series measured simultaneously with a rake of four hot-wires at different transverse positions, each 5 mm apart, in a narrow mixing layer with $B = 30$ mm and $L = 1200$ mm. The nozzle velocity was $U_0 = 8$ m/sec. The test section with adjustable sidewalls is shown in Fig. 1. Typical dimensions are displayed in the sketch. Rake measurements were done at the streamwise positions $x = 200, 400, 600, 800, 1000$ and 1200 mm and at 41 different lateral positions with a resolution of $\Delta y = 10$ mm.

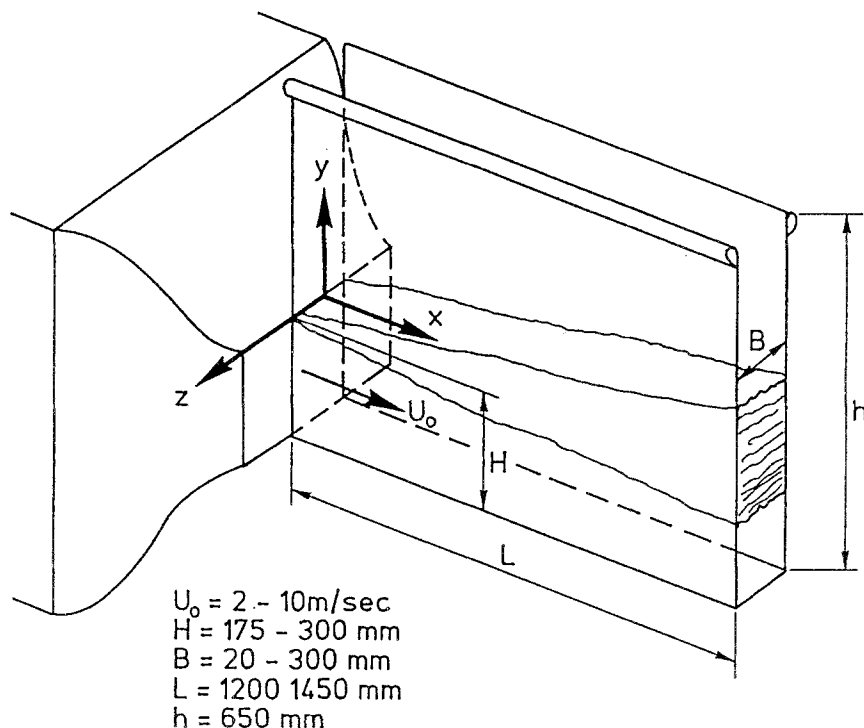


Fig. 1. Sketch of the test section.

Figure 2 shows the distribution of four eigenvalues over the y -axis at different streamwise positions, where b denotes the local width of the shear layer. At all positions the normalized energy content of the first POD mode is significantly higher than that of the other modes, reaching maximum values of 65–90%. This indicates that more than just the periodic energy is captured in the first POD mode. The y -position of the maximum within the mixing layer is identical with the location of the largest periodic fraction.

At streamwise positions close to the splitterplate the first eigenvalue shows a second maximum outside the mixing layer at negative y -positions. Closer inspection shows that the corresponding eigenvectors differ from those within the shear-layer. At positions further downstream this behaviour is no longer observed. The calculated components of the eigenvectors Ξ within the mixing layer have nearly equal distribution for each vector at all streamwise and lateral positions. An example is shown in Fig. 3 for $x = 1000 \text{ mm}$. Small differences of the components of respective eigenvectors at different lateral positions at $x < 400 \text{ mm}$ are vanishing further downstream, being independent of y . Particularly, the components of the first eigenvector are identical also in spanwise direction, which points at the two-dimensionality of the large structures depicted by the first POD mode. This is in agreement with correlation measurements of the periodic part of the turbulent

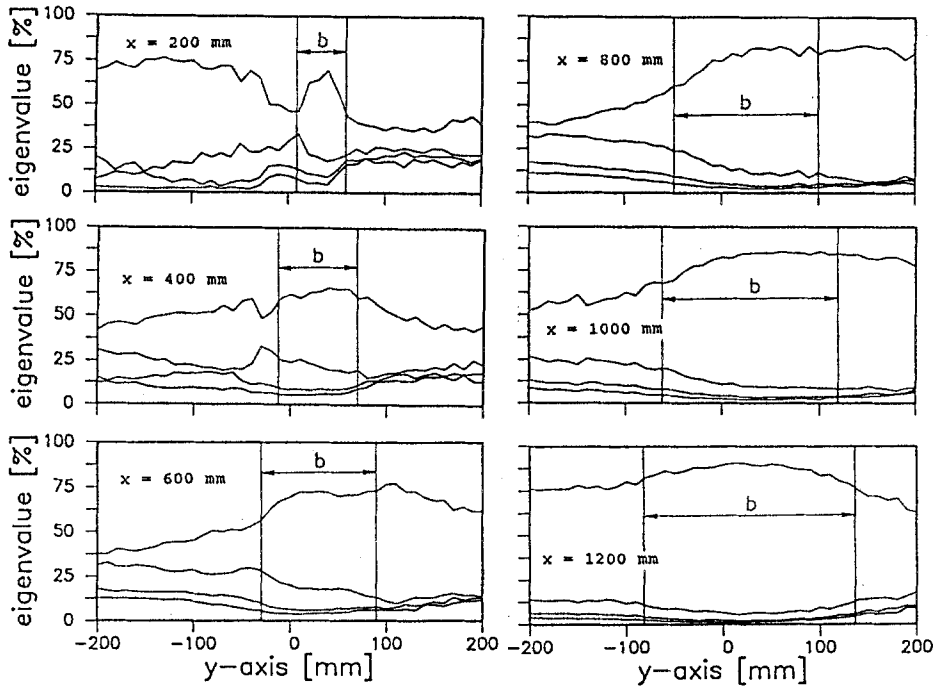


Fig. 2. Eigenvalues at different x -positions as functions of y .

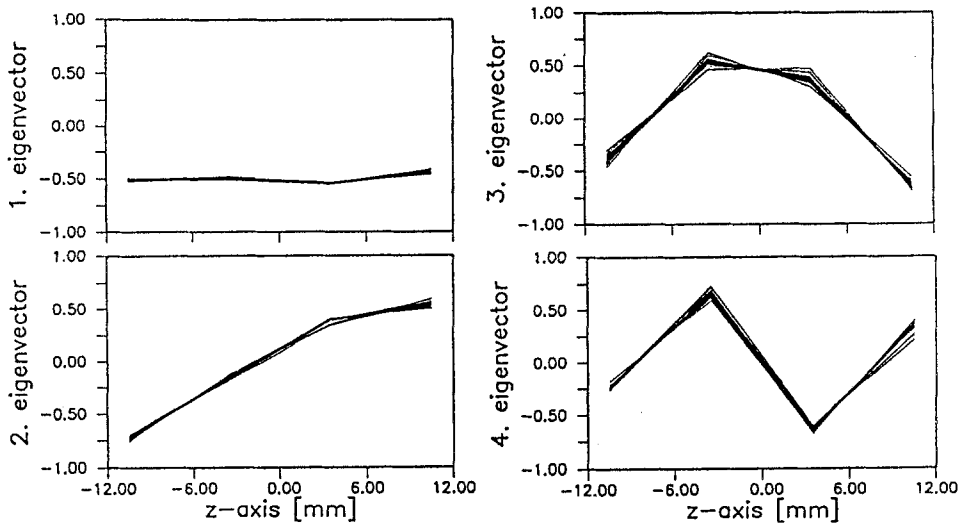


Fig. 3. Eigenvectors at $x = 1000$ mm.

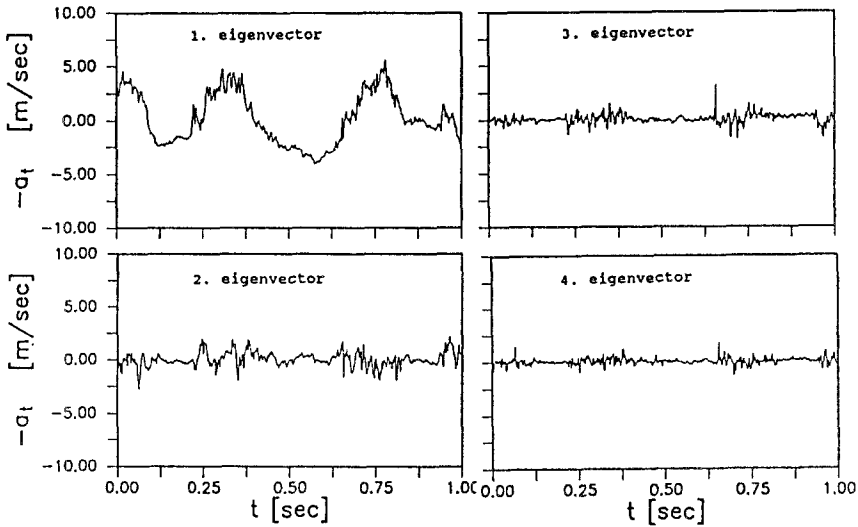


Fig. 4. Coefficients at $x = 1000$ mm.

motion. In relation to the corresponding eigenvalues the two-dimensional fraction of the turbulent fluctuations describes most of the turbulent motion within the narrow shear-layer.

Figure 4 shows the coefficients a_t at $x = 1000$ mm and $y = 40$ mm, where the first eigenvalue has its maximum. The large periodic fraction is found only in the coefficient of the first mode. However, also higher Fourier modes are embedded in this mode, indicating a two-dimensionality of higher spectral fractions. Especially the small scale fluctuations near the maximum of the large scale motion suggest that the small three-dimensional vortices are partly stretched by the large structures, thereby becoming essentially two-dimensional.

The other POD modes include only higher Fourier modes. Obviously, there is a correlation between the phase of the large fluctuation and the amplitude of the motion captured by the higher modes. This is clearly seen in the third and fourth modes, showing the influence of larger structures on the entire turbulent motion. Due to this phenomenon the mixing process in the shear-layer may be different from that in more or less stochastic turbulence. The large vortex rolls up layers of potential fluid from both sides, where the mixing between those is generated by small scale vortices. This is supported by measurements of intermittency, which shows considerably smaller values than those obtained in the wide shear layer.

4. Application of Snapshot POD

For the application of snapshot POD phase-averaged u - and v -data were taken with an X-wire probe in a field of 451 lateral and streamwise positions in the centre

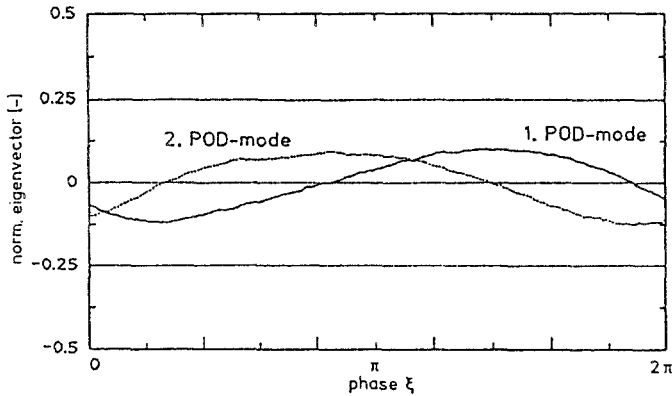


Fig. 5. First and second eigenvector.

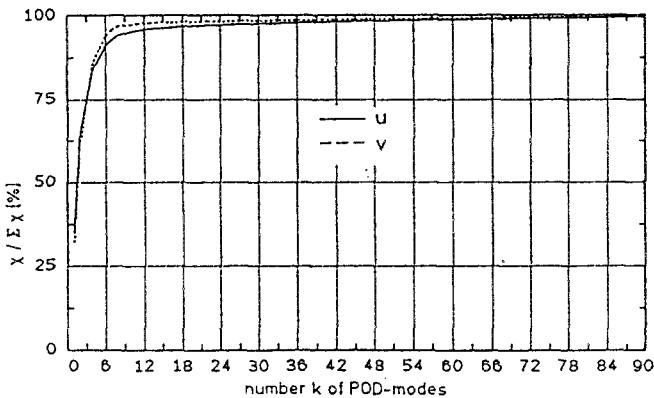


Fig. 6. Eigenvalue distribution.

plane between the sidewalls. The inherent periodicity of the flow was stabilized by weak forcing to simplify the education of data.

A total of 180 snapshots at equidistant phase positions were calculated. The components of corresponding eigenvectors of the u' - and v' -data show strong similarity. The eigenvectors of the first and second mode show the same periodicity of one wavelength, however, with a phase shift of about 180 degrees (Fig. 5). Corresponding normalized eigenvalues reach values of 30%. Higher modes have exponentially decreasing eigenvalues (Fig. 6) and the components of the eigenvectors exhibit smaller wavelengths, decreasing by integer fractions. The first four modes alone describe about 80% of the total energy. According to the previous results of the classical POD analysis, the energy containing modes of the snapshot POD should be two-dimensional. The application of the snapshot POD at other spanwise locations show, that the first four modes are independent of z .

Velocity and streakline plots were calculated from the reconstructed flow field with different numbers of modes. Thus, reconstruction from the first ten modes provides a reconstruction quality of 96%, according to a criterion by Sirovich

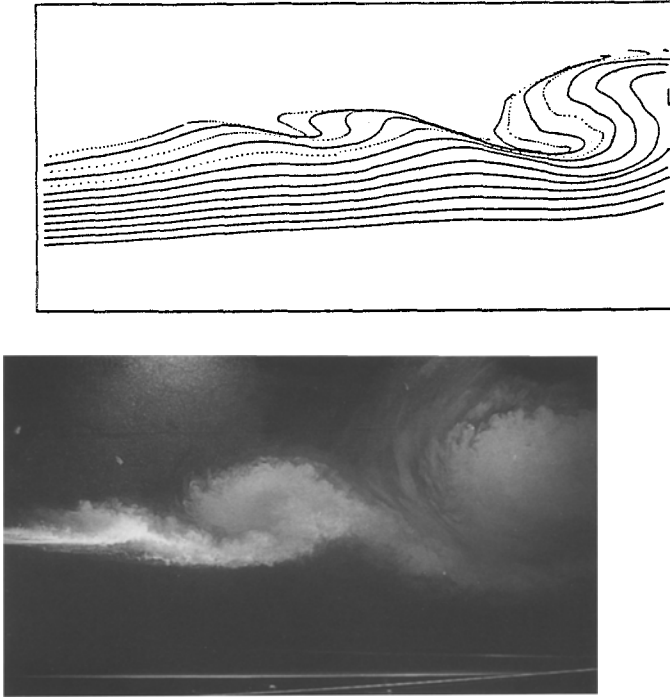


Fig. 7. Streakline reconstruction and flow visualization.

and Kirby (1987). Comparison of streakline plots and flow visualization enables the identification and association of physical patterns to POD modes, showing in particular the largest physical structures to be contained in the first four modes (Fig. 7).

Calculation of the vorticity component $\omega_z \approx -\partial u / \partial y$ of the original and reconstructed velocity field by use of different number of POD modes ($k = 2, 4$ and 180) shows that only 2 of 180 modes contain the largest fraction of coherent vorticity (Fig. 8). Also streakline plots identify the largest visible structure to be represented by only the first two POD modes.

5. Conclusions

Both, classical and snapshot POD, were applied to data measured in a shear-layer with small sidewall distance. The classical POD showed that the major portion, up to 90%, of the turbulent energy within the shear-layer is typically of two-dimensional character. This fraction is described by the first POD mode. This mode includes, however, not only the periodic part of the fluctuation referring to the significant peak in Fourier spectra, but also higher Fourier modes. It was shown, that the coherent physical structures are described by only the first mode. In principle, those results may also be obtained by extracting coherent Fourier modes

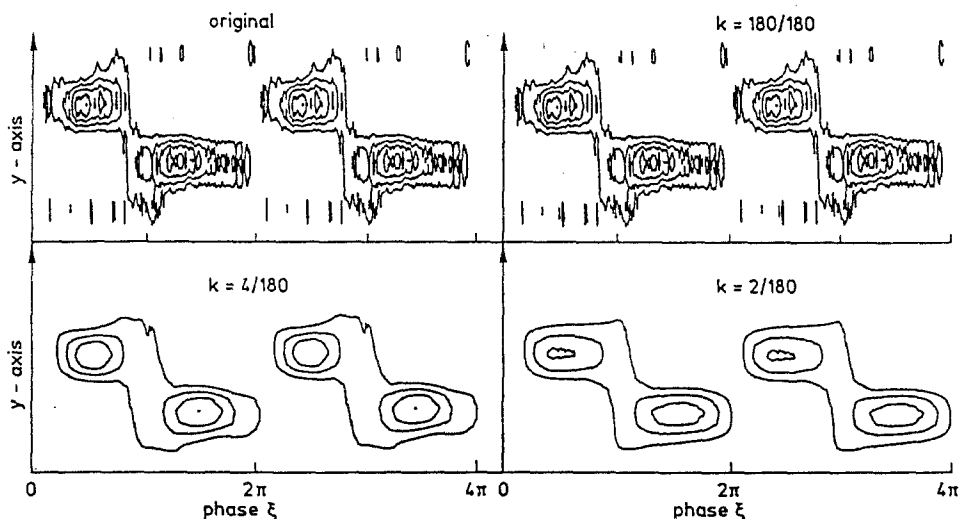


Fig. 8. Comparison of vorticity component, ω_z of original and reconstructed velocity field at $x = L$ as function of phase (POD modes: $k = 2, 4$ and 180).

by correlation calculations. However, the POD does not require pre-information about the correlation functions, so that the computation time is reduced. In contrast to methods requiring a given base, POD is an objective analysis (Lumley, 1981).

Application of snapshot POD on phase-averaged data permits unambiguous separation of modes, which are related to physical patterns. The first four modes contain about 80% of the energy. The reconstructed velocity field from 10 modes out of 180 shows less than 4% overall deviation when compared to the original data. Comparison of streakline plots with flow visualization identifies the first four modes to be included in the typical structure.

References

- Fiedler, H.E. and Hilberg, D., Control of turbulent shear flows via stationary boundary conditions. In *NATO Advances Research Workshop: The Global Geometry of Turbulence* (1992).
- Glezer, A., Kadioglu, Z. and Pearlstein, A.J., Development of an extended proper orthogonal decomposition and its application to a time periodically forced mixing layer. *Physics of Fluids A* (1989) 1363–1373.
- Hilberg, D. and Fiedler, H.E., The spanwise confined mixing layer. In Fernholz and Fiedler (eds), *Advances in Turbulence*, Vol. 2 (1989) pp. 443–448.
- Loeve, M., *Probability Theory*. Van Nostrand (1955).
- Lumley, J.L., The structure of inhomogeneous turbulent flows. In Yaglom and Tatarski (eds), *Atmospheric Turbulence and Radio Wave Propagation* (1967).
- Lumley, J.L., Coherent structures in turbulence. In *Transition and Turbulence* (1981).
- Sirovich, L., Turbulence and the dynamics of coherent structures, parts i–iii. *Quart. J. Appl. Math.* 45 (1987) 561–590.
- Sirovich, L., Chaotic dynamics of coherent structures. *Physica D* 37 (1989) 126–145.
- Sirovich, L. and Kirby, M., Low dimensional procedure for the characterization of human faces. *J. Opt. Soc. Am.* (1987) 519–525.